JACS
JOURNAL OF THE AMERICAN CHEMICAL SOCIETY

Article

Cite This: J. Am. Chem. Soc. 2020, 142, 373−381

pubs.acs.org/JACS

A Small Cationic Organo−Copper Cluster as Thermally Robust Highly Photo- and Electroluminescent Material

Marian Olaru,[†] Elena Rychagova,[‡] Sergey Ketkov,*[,‡] Yevhen Shynkarenko,[§,∥] Sergii Yakunin,[§,∥] Maksym V. Kovalenko,*[,§,∥] Artem Yablonskiy,[#] Boris Andreev,[#] Florian Kleemiss,[†] Jens Beckmann,*[,†] and Matthias Vogt*[,†]

[†]Institut für Anorganische Chemie und Kristallographie, Universität Bremen, Leobener Straße 7, 28359 Bremen, Germany

[‡]G. A. Razuvaev Institute of Organometallic Chemistry, Russian Academy of Sciences, Tropinina, 49, Nizhny Novgorod, 603950, Russian Federation

[§]Laboratory of Inorganic Chemistry, Department of Chemistry and Applied Bioscience, ETH Zürich, Vladimir Prelog Weg 1, CH-8093 Zürich, Switzerland

[∥]Laboratory for Thin Films and Photovoltaics, Empa−Swiss Federal Laboratories for Materials Science and Technology, Überlandstrasse 129, CH-8600 Dübendorf, Switzerland

[#]Institute for Physics of Microstructures, Russian Academy of Sciences, 7 ul. Akademicheskaya, Nizhny Novgorod, 603950, Russian Federation

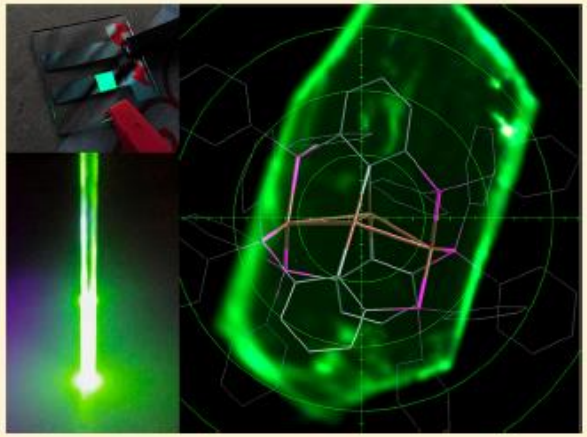

Arijit Jana
20.06.2020

Phosphorescence materials

Organic materials

- Persulfurated derivatives
- fluorene derivatives
- dibenzothiophene and related sulfur-containing heteroaromatic Derivative
- carbazole and related nitrogen-containing heteroaromatic derivatives
- sulfur-nitrogen-containing heteroaromatic derivatives
- Borate derivatives
- polyacid derivatives

Organo-metallic materials

- Iridium based
- Platinum based
- Lanthanides based

Copper based materials

ChemComm *Chem. Commun.*, 1999

Thiacalixarenes as cluster keepers: synthesis and structural analysis of a magnetically coupled tetracopper(II) square

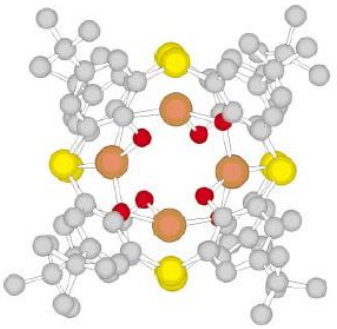

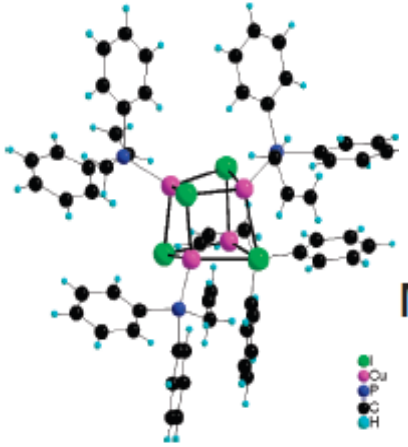

J|A|C|S COMMUNICATIONS

Published on Web 07/26/2010

Mechanochromic and Thermochromic Luminescence of a Copper Iodide Cluster

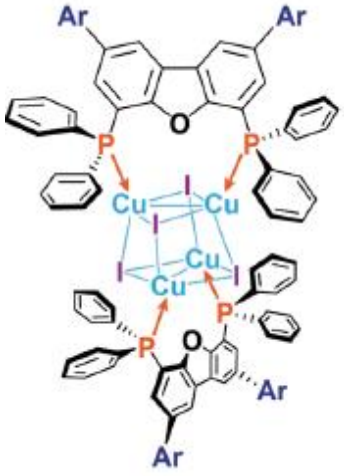

SCIENCE ADVANCES | RESEARCH ARTICLE

Xie *et al.*, *Sci. Adv.* 2019

MATERIALS SCIENCE

Highly efficient sky blue electroluminescence from ligand-activated copper iodide clusters: Overcoming the limitations of cluster light-emitting diodes

❖ Synthesis of the materials:

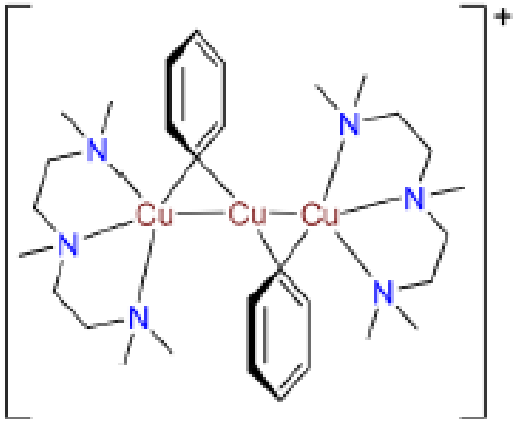

A, Power, 1994

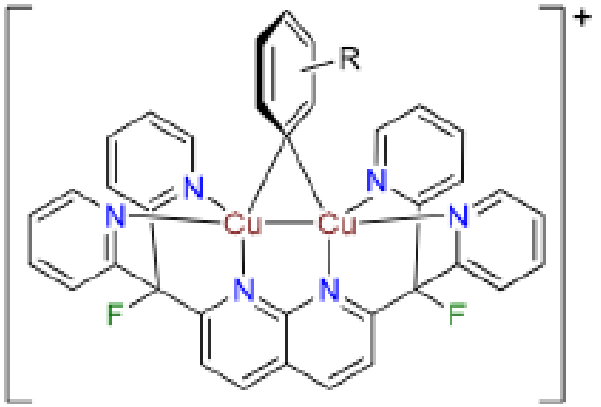

B, Tilley, 2016

This work:

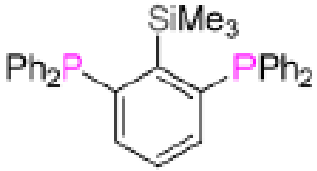

(i) 1.33 eq $[Cu(NCCH_3)_4][BF_4]$
THF, 85°C, 7 d

(ii) optional
$Na[BAr^F{}_4]$
CH_2Cl_2, toluene

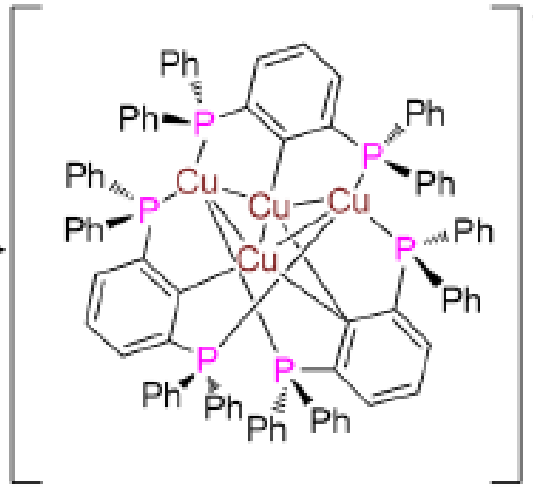

1

(i) A = BF_4, **[2][BF_4]**

(i)+(ii) A = $BAr^F{}_4$, **[2][$BAr^F{}_4$]**, Ar^F = 3,5-$(CF_3)_2C_6H_3$

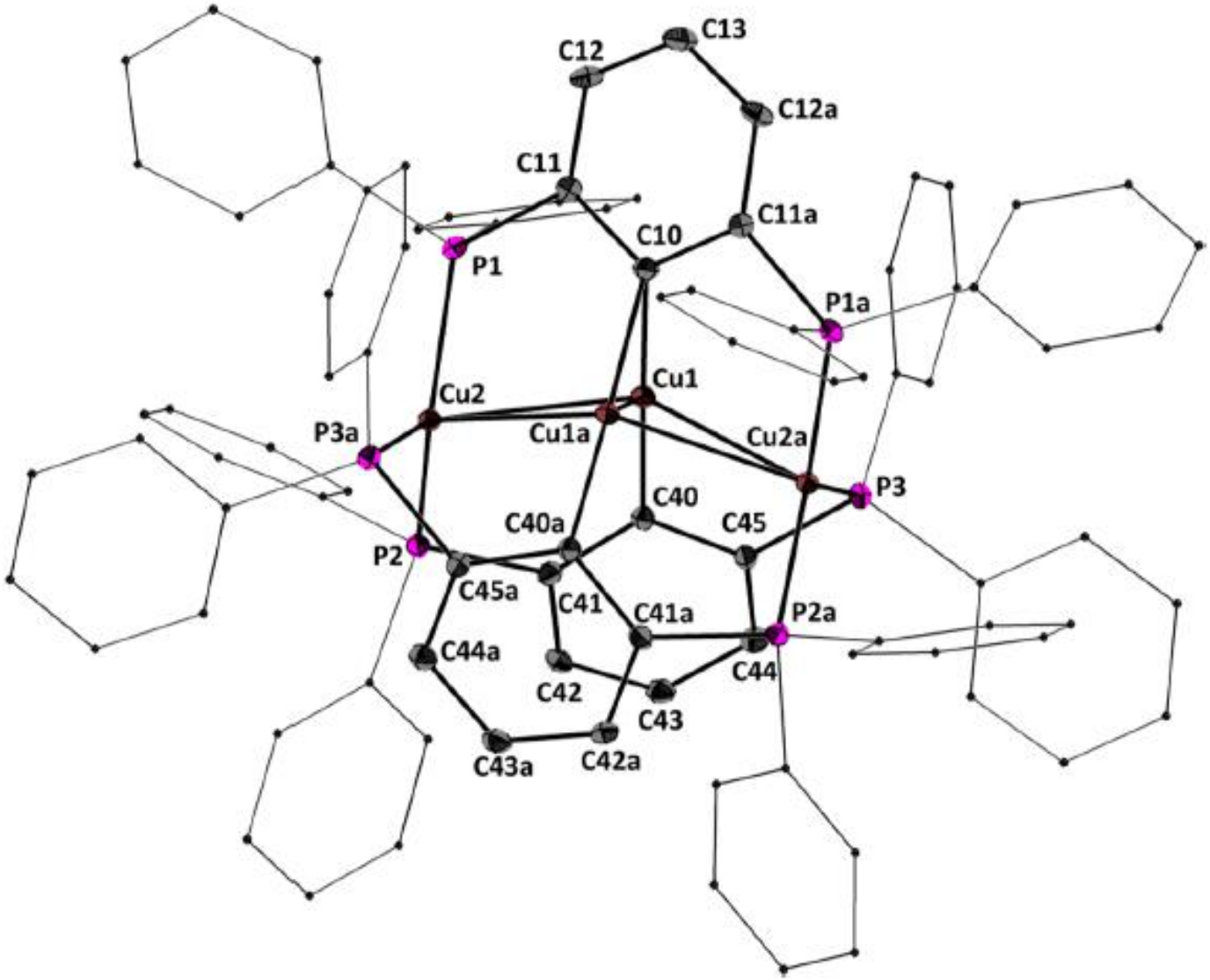

Figure 2. Molecular structure of complex [2][BF_4] derived from single-crystal X-ray diffraction analysis. Hydrogen atoms, CH_2Cl_2 solvent molecule, and $[BF_4]^-$ counterion are omitted for clarity. Ligand scaffold drawn as wire frame; the C of central phenylate units, Cu, and P are depicted as thermal ellipsoids at 30% probability.

Fluxional behavior of the materials:

δ = 12.9, 4.6, and 1.7 ppm ($_2J(_{31}P-_{31}P)$ = 88, 78 Hz)

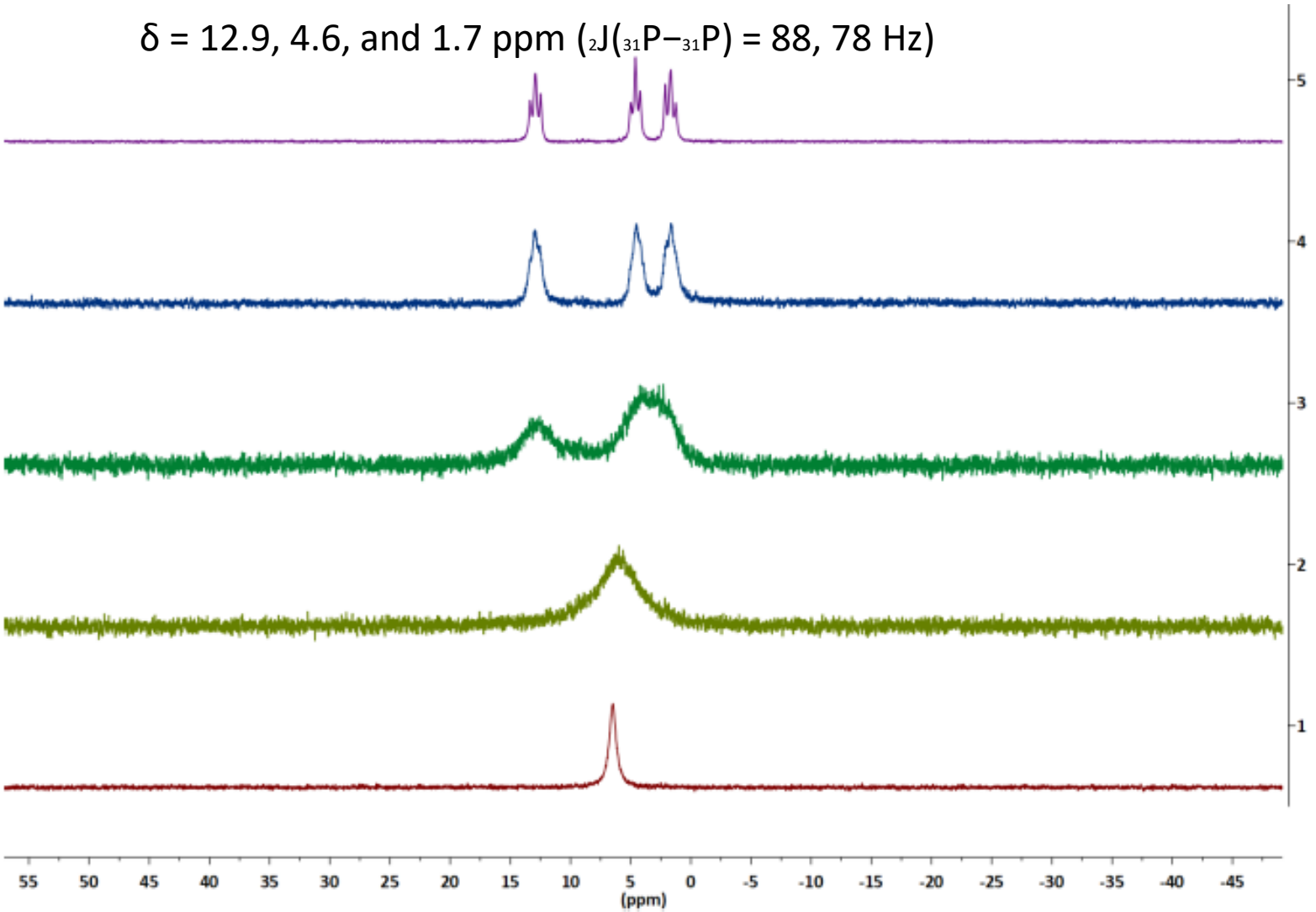

Figure S20. Variable temperature $^{31}P\{^{1}H\}$ NMR (THF-*d8*, 203 MHz) spectra of [**2**][BAr^{F}_{4}]. (1) ^{31}P NMR spectrum at 298.2 K (25.1 °C). (2) ^{31}P NMR spectrum at 273.0 K (−0.2 °C). (3) ^{31}P NMR spectrum at 253.1 K (−20.1 °C). (4) ^{31}P NMR spectrum at 233.1 K (−40.1 °C). (5) ^{31}P NMR spectrum at 223.0 K (−50.2 °C).

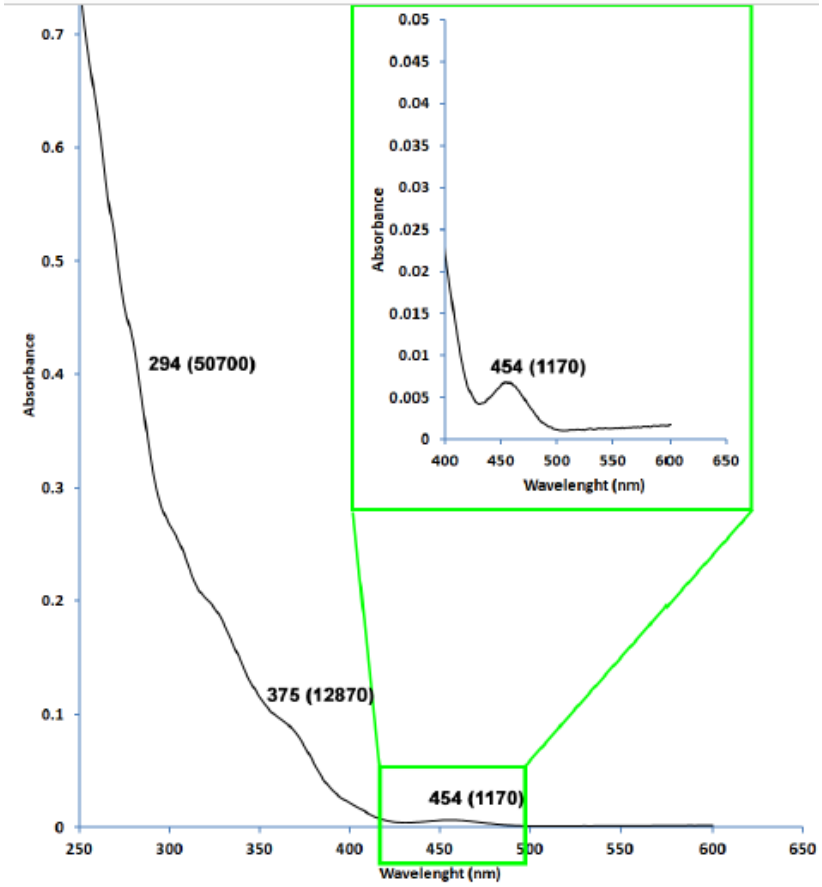

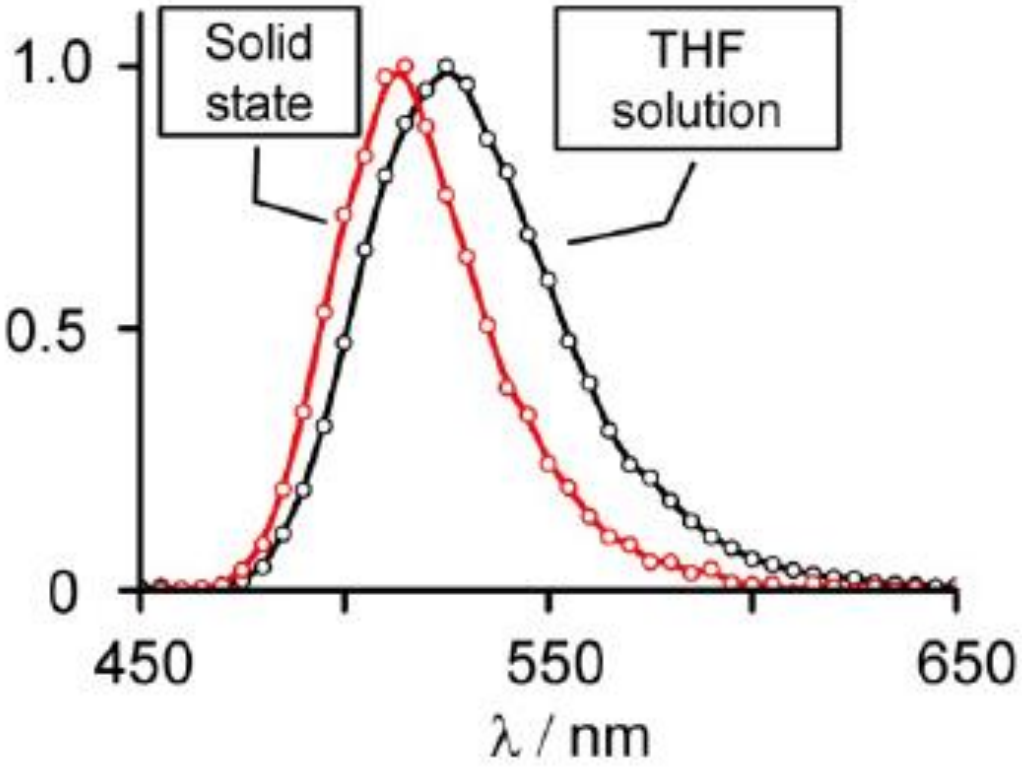

Table S2. PLOY for the solid and (frozen) solutions of [**2**][BAr^F_4] at 298 K and 77 K.

	298 K	**77 K**
Powdered solid	0.50	0.71
DCM solution	0.78	0.93
THF solution	0.79	0.82

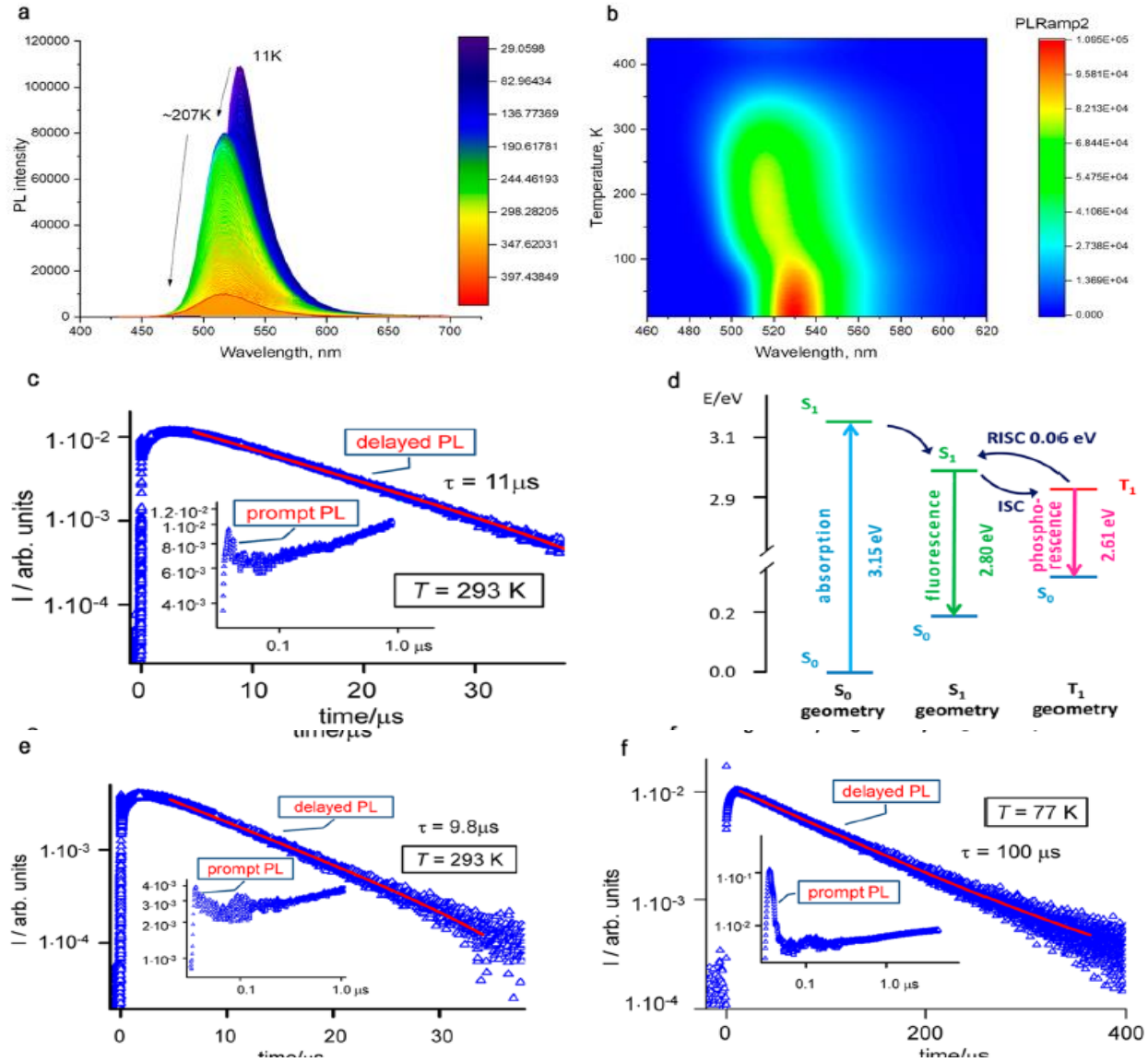

Figure 3. (a and b) Temperature-dependent PL measurement of solid $[Cu_4(PCP)_3][BAr^F{}_4]$: 220 spectra recorded every minute applying a continuous ramp of 2 K min^{-1} (11 K to 450 K with excitation at 390 nm (xenon lamp)). (c) Luminescence kinetics (λ_{ex} = 454 nm) of $[2][BF_4]$ in THF solution at room temperature. Inset shows the initial part of the kinetic curve with the logarithmic time scale. The red line corresponds to the DPL exponential decay model. (d) Quantitative B3LYP/DGDZVP diagram of the electronic states responsible for the photophysical properties of $[2]^+$. The electronic energies were calculated with the optimized geometries of the S_0, S_1, and T_1 states. (e and f) Luminescence kinetics (λ_{ex} = 454 nm) of $[2][BF_4]$ in the solid state at 293 K (e) and 77 K (f). Inset shows the initial part of the kinetic curve with the logarithmic time scale. The red line corresponds to the DPL exponential decay model.

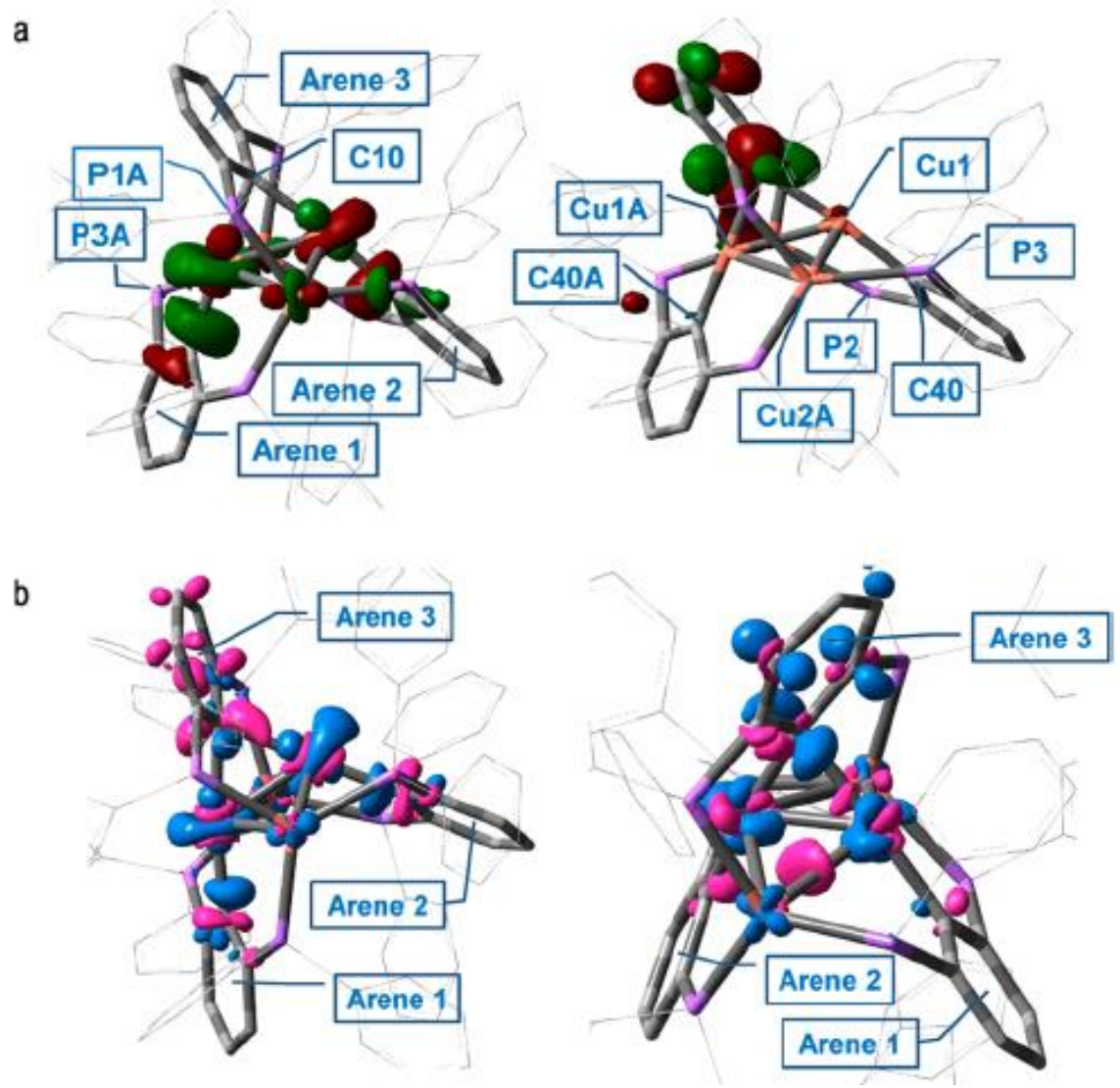

Figure 5. (a) Isosurfaces (isovalue 0.05) of the $[2]^+$ HOMO (left) and LUMO (right) frontier orbitals in the S_0 ground state. (b) Isosurfaces of EDD corresponding to the $S_0 \rightarrow S_1$ vertical transition (left, isovalue is 0.003 au) and $S_1 \rightarrow T_1$ intersystem crossing (right, isovalue is 0.0008 au) in the $[2]^+$ ion. The negative and positive values are shown in blue and rose, respectively.

The ground state molecular structure undergoes, therefore, a larger conformational distortion in the T_1 triplet state as compared to the S_1 singlet.

our DFT calculations provide a detailed description of the CT accompanying the excitation, ISC, and emission processes in the $[2]^+$ ion. The close energies of the S_1 and T_1 states (Figure 3d) allow for the thermally activated population of the S_1 emissive state.

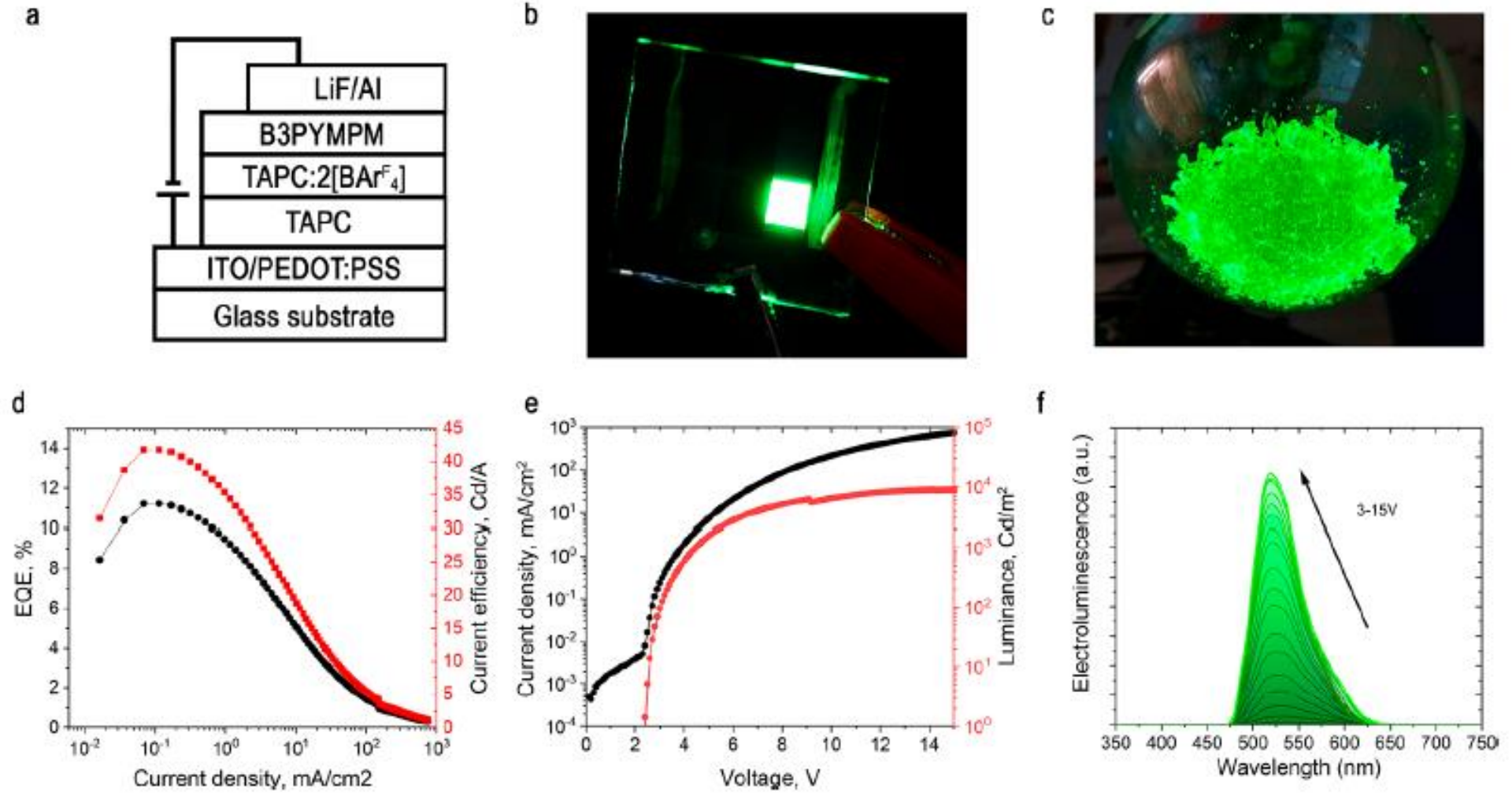

Figure 4. (a) Schematic architecture of the OLED structure. (b) Emission from an OLED prototype with $[2]^+$ as a luminophore. (c) Green emission of crystalline $[2][BAr^F{}_4]$ under UV (254 nm) light exposure. (d) EQE and current efficiency vs current density. (e) Current density–luminance–voltage characteristics of the EL device. (f) EL spectra for various driving voltages.

Conclusion:

a) This paper reports the synthesis of a rare cyclocarbamate protected cationic organocopper cluster compound, [Cu4(PCP)3][A] with good stability.

b) The crystal structure of $[2]^+$ reveals a Cu4 core in rhombic arrangement showing one of the shortest Cu−Cu interatomic distances (2.316(1) Å) reported today.

c) The extraordinary oxidative and thermal stability of [2]+ is a direct result of the efficient Cu4-core steric shielding. Ligand dissociation, exchange, and solvent coordination effects were not observed, and the cluster does not show decomposition before 377 °C.

d) The frontier orbitals are spatially well separated: The HOMO is mainly located at nonbridging Cu−C moieties, and the LUMO on the bridging arene, resulting in a small ΔE(S1−T1) energy gap allowing for the thermally activated population of the S1 emissive state.

e) TADF contribution as 94%, 79% and 0.5% at 300 K, 200 K and 77 K, respectively. These results seem to be reasonable and correlate with the assumption of the 77K emission arising almost entirely from the T1 phosphorescence.

f) Cluster was utilized as a solution-processed dopant in the emissive layer for OLED devices.